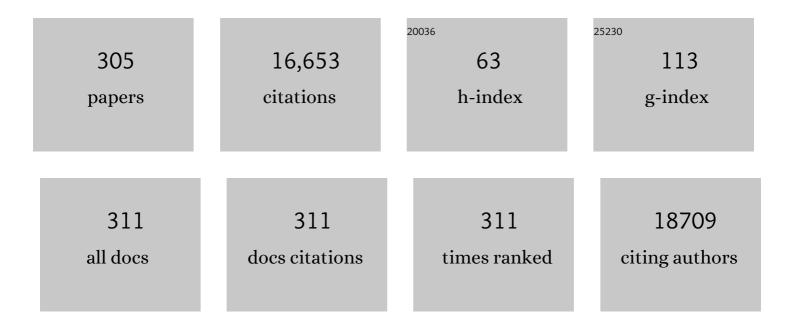
Andrew H -J Wang

List of Publications by Year in descending order

Source: https://exaly.com/author-pdf/2402357/publications.pdf Version: 2024-02-01



#	Article	IF	CITATIONS
1	Structural basis of an epitope tagging system derived from <i>Haloarcula marismortui</i> bacteriorhodopsin I D94N and its monoclonal antibody GDâ€26. FEBS Journal, 2022, 289, 730-747.	2.2	1
2	Structural and biological insights into Klebsiella pneumoniae surface polysaccharide degradation by a bacteriophage K1 lyase: implications for clinical use. Journal of Biomedical Science, 2022, 29, 9.	2.6	9
3	Biosynthesis of Vitroprocines by α-Oxoamine Synthase and Oxidoreductase Identified from <i>Vibrio</i> sp. QWI-06. Organic Letters, 2022, 24, 3281-3285.	2.4	0
4	Structure, catalysis, and inhibition mechanism of prenyltransferase. IUBMB Life, 2021, 73, 40-63.	1.5	34
5	How does <scp>the International Union of Biochemistry and Molecular Biology</scp> support education and training?. Biochemistry and Molecular Biology Education, 2021, 49, 7-8.	0.5	Ο
6	Crystal structure of the N-terminal domain of TagH reveals a potential drug targeting site. Biochemical and Biophysical Research Communications, 2021, 536, 1-6.	1.0	1
7	Structure-based Development of Human Interleukin-1β-Specific Antibody That Simultaneously Inhibits Binding to Both IL-1RI and IL-1RAcP. Journal of Molecular Biology, 2021, 433, 166766.	2.0	10
8	DMTMM-Mediated Intramolecular Cyclization of Acidic Residues in Peptides/Proteins. ACS Omega, 2021, 6, 4708-4718.	1.6	1
9	Concern over use of the term Z-DNA. Nature, 2021, 594, 333-333.	13.7	2
10	A Unique Carboxylic-Acid Hydrogen-Bond Network (CAHBN) Confers Glutaminyl Cyclase Activity on M28 Family Enzymes. Journal of Molecular Biology, 2021, 433, 166960.	2.0	1
11	Synthesis and biological evaluation of phenothiazine derivative-containing hydroxamic acids as potent class II histone deacetylase inhibitors. European Journal of Medicinal Chemistry, 2021, 219, 113419.	2.6	8
12	<scp>IUBMB</scp> Life enters a new era. IUBMB Life, 2021, 73, 9-9.	1.5	0
13	Vibrio cholerae biofilm scaffolding protein RbmA shows an intrinsic, phosphateâ€dependent autoproteolysis activity. IUBMB Life, 2021, 73, 418-431.	1.5	2
14	Structural basis of polyethylene glycol recognition by antibody. Journal of Biomedical Science, 2020, 27, 12.	2.6	34
15	Preparation and characterization of antibody-drug conjugates acting on HER2-positive cancer cells. PLoS ONE, 2020, 15, e0239813.	1.1	9
16	Biochemical and molecular dynamics studies of archaeal polyisoprenyl pyrophosphate phosphatase from Saccharolobus solfataricus. Enzyme and Microbial Technology, 2020, 139, 109585.	1.6	2
17	Development of a Versatile and Modular Linker for Antibody–Drug Conjugates Based on Oligonucleotide Strand Pairing. Bioconjugate Chemistry, 2020, 31, 1804-1811.	1.8	9
18	Crystal Structure of PigA: A Prolyl Thioesterâ€Oxidizing Enzyme in Prodigiosin Biosynthesis. ChemBioChem, 2019, 20, 193-202.	1.3	7

#	Article	IF	CITATIONS
19	Enhancement of laccase activity by pre-incubation with organic solvents. Scientific Reports, 2019, 9, 9754.	1.6	35
20	Chaetomella raphigera Î ² -glucosidase D2-BGL has intriguing structural features and a high substrate affinity that renders it an efficient cellulase supplement for lignocellulosic biomass hydrolysis. Biotechnology for Biofuels, 2019, 12, 258.	6.2	19
21	Thermococcus sp. 9°N DNA polymerase exhibits 3′-esterase activity that can be harnessed for DNA sequencing. Communications Biology, 2019, 2, 224.	2.0	6
22	An Effective Neutralizing Antibody Against Influenza Virus H1N1 from Human B Cells. Scientific Reports, 2019, 9, 4546.	1.6	13
23	Crystal Structures of the Câ€Terminally Truncated Endoglucanase Cel9Q from <i>Clostridium thermocellum</i> Complexed with Cellodextrins and Tris. ChemBioChem, 2019, 20, 295-307.	1.3	4
24	New paradigm of functional regulation by DNA mimic proteins: Recent updates. IUBMB Life, 2019, 71, 539-548.	1.5	24
25	Antibody-drug conjugates with HER2-targeting antibodies from synthetic antibody libraries are highly potent against HER2-positive human gastric tumor in xenograft models. MAbs, 2019, 11, 153-165.	2.6	10
26	The C-terminal D/E-rich domain of MBD3 is a putative Z-DNA mimic that competes for Zα DNA-binding activity. Nucleic Acids Research, 2018, 46, 11806-11821.	6.5	6
27	Kinetic analysis and structural studies of a highâ€efficiency laccase from <i>Cerrena</i> sp. <scp>RSD</scp> 1. FEBS Open Bio, 2018, 8, 1230-1246.	1.0	20
28	Structural Basis for Stabilization of Z-DNA by Cobalt Hexaammine and Magnesium Cations. journal of hand surgery Asian-Pacific volume, The, 2018, , 196-199.	0.2	0
29	Molecular structure of a left-handed double helical DNA fragment at atomic resolution. journal of hand surgery Asian-Pacific volume, The, 2018, , 180-186.	0.2	0
30	Structural basis for fragmenting the exopolysaccharide of Acinetobacter baumannii by bacteriophage ΦAB6 tailspike protein. Scientific Reports, 2017, 7, 42711.	1.6	49
31	Crystal Structure and Potential Head-to-Middle Condensation Function of a <i>Z</i> , <i>Z</i> -Farnesyl Diphosphate Synthase. ACS Omega, 2017, 2, 930-936.	1.6	23
32	In search of tail-anchored protein machinery in plants: reevaluating the role of arsenite transporters. Scientific Reports, 2017, 7, 46022.	1.6	8
33	Expression, purification and enzymatic characterization of undecaprenyl pyrophosphate phosphatase from Vibrio vulnificus. Protein Expression and Purification, 2017, 133, 121-131.	0.6	4
34	High throughput discovery of influenza virus neutralizing antibodies from phage-displayed synthetic antibody libraries. Scientific Reports, 2017, 7, 14455.	1.6	15
35	The Arginine Pairs and C-Termini of the Sso7c4 from Sulfolobus solfataricus Participate in Binding and Bending DNA. PLoS ONE, 2017, 12, e0169627.	1.1	4
36	Exploring the Mechanism Responsible for Cellulase Thermostability by Structure-Guided Recombination. PLoS ONE, 2016, 11, e0147485.	1.1	32

#	Article	IF	CITATIONS
37	Moenomycin Biosynthesis: Structure and Mechanism of Action of the Prenyltransferase MoeN5. Angewandte Chemie - International Edition, 2016, 55, 4716-4720.	7.2	19
38	High throughput cytotoxicity screening of anti-HER2 immunotoxins conjugated with antibody fragments from phage-displayed synthetic antibody libraries. Scientific Reports, 2016, 6, 31878.	1.6	19
39	Crystal structure of vespid phospholipase A1 reveals insights into the mechanism for cause of membrane dysfunction. Insect Biochemistry and Molecular Biology, 2016, 68, 79-88.	1.2	18
40	Using structural-based protein engineering to modulate the differential inhibition effects of SAUGI on human and HSV uracil DNA glycosylase. Nucleic Acids Research, 2016, 44, 4440-4449.	6.5	14
41	Determining the N-terminal orientations of recombinant transmembrane proteins in the Escherichia coli plasma membrane. Scientific Reports, 2015, 5, 15086.	1.6	11
42	Chromophore Deprotonation State Alters the Optical Properties of Blue Chromoprotein. PLoS ONE, 2015, 10, e0134108.	1.1	6
43	Structural D/E-rich repeats play multiple roles especially in gene regulation through DNA/RNA mimicry. Molecular BioSystems, 2015, 11, 2144-2151.	2.9	46
44	Predominant structural configuration of natural antibody repertoires enables potent antibody responses against protein antigens. Scientific Reports, 2015, 5, 12411.	1.6	17
45	Specificity of the ModA11, ModA12 and ModD1 epigenetic regulator N6-adenine DNA methyltransferases of Neisseria meningitidis. Nucleic Acids Research, 2015, 43, 4150-4162.	6.5	58
46	Substrate Specificity and Plasticity of FERM-Containing Protein Tyrosine Phosphatases. Structure, 2015, 23, 653-664.	1.6	20
47	Structural and Functional Studies of a Newly Grouped Haloquadratum walsbyi Bacteriorhodopsin Reveal the Acid-resistant Light-driven Proton Pumping Activity. Journal of Biological Chemistry, 2015, 290, 29567-29577.	1.6	13
48	In situ proteolysis of the <i>Vibrio cholerae</i> matrix protein RbmA promotes biofilm recruitment. Proceedings of the National Academy of Sciences of the United States of America, 2015, 112, 10491-10496.	3.3	48
49	The opportunistic marine pathogen <i>Vibrio parahaemolyticus</i> becomes virulent by acquiring a plasmid that expresses a deadly toxin. Proceedings of the National Academy of Sciences of the United States of America, 2015, 112, 10798-10803.	3.3	427
50	Crystal structures of ligandâ€bound octaprenyl pyrophosphate synthase from <i>Escherichia coli</i> reveal the catalytic and chainâ€length determining mechanisms. Proteins: Structure, Function and Bioinformatics, 2015, 83, 37-45.	1.5	22
51	Structural and Functional Roles of Glycosylation in Fungal Laccase from Lentinus sp PLoS ONE, 2015, 10, e0120601.	1.1	67
52	Linked Production of Pyroglutamate-Modified Proteins via Self-Cleavage of Fusion Tags with TEV Protease and Autonomous N-Terminal Cyclization with Glutaminyl Cyclase In Vivo. PLoS ONE, 2014, 9, e94812.	1.1	21
53	Crowning Proteins: Modulating the Protein Surface Properties using Crown Ethers. Angewandte Chemie - International Edition, 2014, 53, 13054-13058.	7.2	49
54	Pin1-mediated Sp1 phosphorylation by CDK1 increases Sp1 stability and decreases its DNA-binding activity during mitosis. Nucleic Acids Research, 2014, 42, 13573-13587.	6.5	19

#	Article	IF	CITATIONS
55	Distinct structural features of Rex-family repressors to sense redox levels in anaerobes and aerobes. Journal of Structural Biology, 2014, 188, 195-204.	1.3	20
56	Squalene Synthase As a Target for Chagas Disease Therapeutics. PLoS Pathogens, 2014, 10, e1004114.	2.1	64
57	Proposed Carrier Lipid-binding Site of Undecaprenyl Pyrophosphate Phosphatase from Escherichia coli. Journal of Biological Chemistry, 2014, 289, 18719-18735.	1.6	36
58	Structural insights into the catalytic mechanism of human squalene synthase. Acta Crystallographica Section D: Biological Crystallography, 2014, 70, 231-241.	2.5	40
59	Staphylococcus aureus protein SAUGI acts as a uracil-DNA glycosylase inhibitor. Nucleic Acids Research, 2014, 42, 1354-1364.	6.5	32
60	TcaR–ssDNA complex crystal structure reveals new DNA binding mechanism of the MarR family proteins. Nucleic Acids Research, 2014, 42, 5314-5321.	6.5	9
61	Structure and Inhibition of Tuberculosinol Synthase and Decaprenyl Diphosphate Synthase from <i>Mycobacterium tuberculosis</i> . Journal of the American Chemical Society, 2014, 136, 2892-2896.	6.6	37
62	Coreâ€shell structure microcapsules with dual pHâ€responsive drug release function. Electrophoresis, 2014, 35, 2673-2680.	1.3	23
63	Crystal structure and substrate-binding mode of the mycoestrogen-detoxifying lactonase ZHD from Clonostachys rosea. RSC Advances, 2014, 4, 62321-62325.	1.7	37
64	Structural Insights into Enzymatic Degradation of Oxidized Polyvinyl Alcohol. ChemBioChem, 2014, 15, 1882-1886.	1.3	18
65	The T4 Phage DNA Mimic Protein Arn Inhibits the DNA Binding Activity of the Bacterial Histone-like Protein H-NS. Journal of Biological Chemistry, 2014, 289, 27046-27054.	1.6	28
66	DNA Mimic Proteins: Functions, Structures, and Bioinformatic Analysis. Biochemistry, 2014, 53, 2865-2874.	1.2	46
67	Structural and functional analyses of a glutaminyl cyclase from <i>Ixodes scapularis</i> reveal metal-independent catalysis and inhibitor binding. Acta Crystallographica Section D: Biological Crystallography, 2014, 70, 789-801.	2.5	10
68	Reciprocal allosteric regulation of p38γ and PTPN3 involves a PDZ domain–modulated complex formation. Science Signaling, 2014, 7, ra98.	1.6	25
69	Structural Insights of the ssDNA Binding Site in the Multifunctional Endonuclease AtBFN2 from Arabidopsis thaliana. PLoS ONE, 2014, 9, e105821.	1.1	7
70	Mechanistic insights to catalysis by a zinc-dependent bi-functional nuclease from Arabidopsis thaliana. Biocatalysis and Agricultural Biotechnology, 2013, 2, 191-195.	1.5	5
71	Crystal structure of a Trimeresurus mucrosquamatus venom metalloproteinase providing new insights into the inhibition by endogenous tripeptide inhibitors. Toxicon, 2013, 71, 140-146.	0.8	11
72	Electrostatic droplets assisted in situ synthesis of superparamagnetic chitosan microparticles for magnetic-responsive controlled drug release and copper ion removal. Journal of Materials Chemistry B, 2013, 1, 2205.	2.9	30

#	Article	IF	CITATIONS
73	Using Haloarcula marismortui Bacteriorhodopsin as a Fusion Tag for Enhancing and Visible Expression of Integral Membrane Proteins in Escherichia coli. PLoS ONE, 2013, 8, e56363.	1.1	33
74	Neisseria conserved hypothetical protein DMP12 is a DNA mimic that binds to histone-like HU protein. Nucleic Acids Research, 2013, 41, 5127-5138.	6.5	16
75	Crystal Structure of Vaccinia Viral A27 Protein Reveals a Novel Structure Critical for Its Function and Complex Formation with A26 Protein. PLoS Pathogens, 2013, 9, e1003563.	2.1	32
76	Structural basis for the antibody neutralization of <i>Herpes simplex virus</i> . Acta Crystallographica Section D: Biological Crystallography, 2013, 69, 1935-1945.	2.5	38
77	Structural Insights into RbmA, a Biofilm Scaffolding Protein of V. Cholerae. PLoS ONE, 2013, 8, e82458.	1.1	34
78	The role of protein glycosylation in laccases from Lentinus sp FASEB Journal, 2013, 27, 561.9.	0.2	0
79	Mutations in the substrate entrance region of Â-glucosidase from Trichoderma reesei improve enzyme activity and thermostability. Protein Engineering, Design and Selection, 2012, 25, 733-740.	1.0	81
80	Intermolecular Binding between TIFA-FHA and TIFA-pT Mediates Tumor Necrosis Factor Alpha Stimulation and NF-κB Activation. Molecular and Cellular Biology, 2012, 32, 2664-2673.	1.1	43
81	Binding Modes of Zaragozic Acid A to Human Squalene Synthase and Staphylococcal Dehydrosqualene Synthase. Journal of Biological Chemistry, 2012, 287, 18750-18757.	1.6	39
82	Facile Synthesis of Radial-Like Macroporous Superparamagnetic Chitosan Spheres with In-Situ Co-Precipitation and Gelation of Ferro-Gels. PLoS ONE, 2012, 7, e49329.	1.1	23
83	Neisseria conserved protein DMP19 is a DNA mimic protein that prevents DNA binding to a hypothetical nitrogen-response transcription factor. Nucleic Acids Research, 2012, 40, 5718-5730.	6.5	26
84	Inhibition of glutaminyl cyclase attenuates cell migration modulated by monocyte chemoattractant proteins. Biochemical Journal, 2012, 442, 403-412.	1.7	20
85	Engineering of dual-functional hybrid glucanases. Protein Engineering, Design and Selection, 2012, 25, 771-780.	1.0	10
86	Back Cover: Insights into the Mechanism of the Antibiotic-Synthesizing Enzyme MoeO5 from Crystal Structures of Different Complexes (Angew. Chem. Int. Ed. 17/2012). Angewandte Chemie - International Edition, 2012, 51, 4240-4240.	7.2	0
87	Enhanced activity of Thermotoga maritima cellulase 12A by mutating a unique surface loop. Applied Microbiology and Biotechnology, 2012, 95, 661-669.	1.7	34
88	Structure-based development of bacterial nitroreductase against nitrobenzodiazepine-induced hypnosis. Biochemical Pharmacology, 2012, 83, 1690-1699.	2.0	13
89	High-resolution structures of <i>Neotermes koshunensis</i> β-glucosidase mutants provide insights into the catalytic mechanism and the synthesis of glucoconjugates. Acta Crystallographica Section D: Biological Crystallography, 2012, 68, 829-838.	2.5	36
90	Functional Studies of ssDNA Binding Ability of MarR Family Protein TcaR from Staphylococcus epidermidis. PLoS ONE, 2012, 7, e45665.	1.1	6

#	Article	IF	CITATIONS
91	Structural and functional analysis of three β-glucosidases from bacterium Clostridium cellulovorans, fungus Trichoderma reesei and termite Neotermes koshunensis. Journal of Structural Biology, 2011, 173, 46-56.	1.3	161
92	Conformational change upon product binding to Klebsiella pneumoniae UDP-glucose dehydrogenase: A possible inhibition mechanism for the key enzyme in polymyxin resistance. Journal of Structural Biology, 2011, 175, 300-310.	1.3	20
93	The Hexameric Structures of Human Heat Shock Protein 90. PLoS ONE, 2011, 6, e19961.	1.1	53
94	A Novel Tetrameric PilZ Domain Structure from Xanthomonads. PLoS ONE, 2011, 6, e22036.	1.1	20
95	The many blades of the β-propeller proteins: conserved but versatile. Trends in Biochemical Sciences, 2011, 36, 553-561.	3.7	158
96	Crystal structure and substrateâ€binding mode of cellulase 12A from <i>Thermotoga maritima</i> . Proteins: Structure, Function and Bioinformatics, 2011, 79, 1193-1204.	1.5	37
97	Structure and mechanism of <i>Escherichia coli</i> glutathionylspermidine amidase belonging to the family of cysteine; histidineâ€dependent amidohydrolases/peptidases. Protein Science, 2011, 20, 557-566.	3.1	9
98	Structure and Mechanism of an Arabidopsis Medium/Long-Chain-Length Prenyl Pyrophosphate Synthase Â. Plant Physiology, 2011, 155, 1079-1090.	2.3	68
99	Structures of Human Golgi-resident Glutaminyl Cyclase and Its Complexes with Inhibitors Reveal a Large Loop Movement upon Inhibitor Binding. Journal of Biological Chemistry, 2011, 286, 12439-12449.	1.6	50
100	Terpyridine Platinum(II) Complexes Inhibit Cysteine Proteases by Binding to Active-site Cysteine. Journal of Biomolecular Structure and Dynamics, 2011, 29, 267-282.	2.0	16
101	Modulation of Substrate Specificities of d-Sialic Acid Aldolase through Single Mutations of Val-251. Journal of Biological Chemistry, 2011, 286, 14057-14064.	1.6	10
102	Crystal Structures of the Laminarinase Catalytic Domain from Thermotoga maritima MSB8 in Complex with Inhibitors. Journal of Biological Chemistry, 2011, 286, 45030-45040.	1.6	35
103	The DNA-recognition fold of Sso7c4 suggests a new member of SpoVT-AbrB superfamily from archaea. Nucleic Acids Research, 2011, 39, 6764-6774.	6.5	14
104	Binding and catalysis of <i>Humulus lupulus</i> adenylate isopentenyltransferase for the synthesis of isopentenylated diadenosine polyphosphates. FEBS Letters, 2010, 584, 4083-4088.	1.3	4
105	Structural Basis of αâ€Fucosidase Inhibition by Iminocyclitols with <i>K</i> _i Values in the Micro―to Picomolar Range. Angewandte Chemie - International Edition, 2010, 49, 337-340.	7.2	36
106	The dimeric transmembrane domain of prolyl dipeptidase DPPâ€₩ contributes to its quaternary structure and enzymatic activities. Protein Science, 2010, 19, 1627-1638.	3.1	29
107	Studying submicrosecond protein folding kinetics using a photolabile caging strategy and timeâ€resolved photoacoustic calorimetry. Proteins: Structure, Function and Bioinformatics, 2010, 78, 2973-2983.	1.5	8
108	A 3D Model of the Membrane Protein Complex Formed by the White Spot Syndrome Virus Structural Proteins. PLoS ONE, 2010, 5, e10718.	1.1	71

#	Article	IF	CITATIONS
109	Structure of a Heterotetrameric Geranyl Pyrophosphate Synthase from Mint (<i>Mentha piperita</i>) Reveals Intersubunit Regulation Â. Plant Cell, 2010, 22, 454-467.	3.1	85
110	Mechanism of action and inhibition of dehydrosqualene synthase. Proceedings of the National Academy of Sciences of the United States of America, 2010, 107, 21337-21342.	3.3	66
111	A rationally designed peptide enhances homologous recombination in vitro and resistance to DNA damaging agents in vivo. Nucleic Acids Research, 2010, 38, 4361-4371.	6.5	Ο
112	Crystal structure and substrate specificity of plant adenylate isopentenyltransferase from Humulus lupulus: distinctive binding affinity for purine and pyrimidine nucleotides. Nucleic Acids Research, 2010, 38, 1738-1748.	6.5	16
113	Protein S-Thiolation by Glutathionylspermidine (Gsp). Journal of Biological Chemistry, 2010, 285, 25345-25353.	1.6	35
114	Structural study of TcaR and its complexes with multiple antibiotics from <i>Staphylococcus epidermidis</i> . Proceedings of the National Academy of Sciences of the United States of America, 2010, 107, 8617-8622.	3.3	79
115	Flavin-containing reductase: new perspective on the detoxification of nitrobenzodiazepine. Expert Opinion on Drug Metabolism and Toxicology, 2010, 6, 967-981.	1.5	7
116	Glycan Array on Aluminum Oxide-Coated Glass Slides through Phosphonate Chemistry. Journal of the American Chemical Society, 2010, 132, 13371-13380.	6.6	58
117	Conformational changes associated with cofactor/substrate binding of 6-phosphogluconate dehydrogenase from Escherichia coli and Klebsiella pneumoniae: Implications for enzyme mechanism. Journal of Structural Biology, 2010, 169, 25-35.	1.3	33
118	The cAMP Receptor-Like Protein CLP Is a Novel c-di-GMP Receptor Linking Cell–Cell Signaling to Virulence Gene Expression in Xanthomonas campestris. Journal of Molecular Biology, 2010, 396, 646-662.	2.0	191
119	Crystal Structure and Functional Analysis of the Glutaminyl Cyclase from Xanthomonas campestris. Journal of Molecular Biology, 2010, 401, 374-388.	2.0	23
120	Enhanced Specificity of Mint Geranyl Pyrophosphate Synthase by Modifying the R-Loop Interactions. Journal of Molecular Biology, 2010, 404, 859-873.	2.0	4
121	Three New Structures of Left-Handed RadA Helical Filaments: Structural Flexibility of N-Terminal Domain Is Critical for Recombinase Activity. PLoS ONE, 2009, 4, e4890.	1.1	15
122	Phasevarions Mediate Random Switching of Gene Expression in Pathogenic Neisseria. PLoS Pathogens, 2009, 5, e1000400.	2.1	170
123	Structural Basis of Inhibition Specificities of 3C and 3C-like Proteases by Zinc-coordinating and Peptidomimetic Compounds. Journal of Biological Chemistry, 2009, 284, 7646-7655.	1.6	125
124	Structure, Assembly, and Mechanism of a PLP-Dependent Dodecameric l-Aspartate Î ² -Decarboxylase. Structure, 2009, 17, 517-529.	1.6	22
125	Characterization of Escherichia coli nitroreductase NfsB in the metabolism of nitrobenzodiazepines. Biochemical Pharmacology, 2009, 78, 96-103.	2.0	18
126	Structural bioinformatics analysis of free cysteines in protein environments. Journal of the Taiwan Institute of Chemical Engineers, 2009, 40, 123-129.	2.7	6

#	Article	IF	CITATIONS
127	Crystal structure of RecX: A potent regulatory protein of RecA from <i>Xanthomonas campestris</i> . Proteins: Structure, Function and Bioinformatics, 2009, 74, 530-537.	1.5	6
128	XC1028 from <i>Xanthomonas campestris</i> adopts a PilZ domainâ€like structure without a câ€diâ€GMP switch. Proteins: Structure, Function and Bioinformatics, 2009, 75, 282-288.	1.5	43
129	Terpyridine–platinum(II) complexes are effective inhibitors of mammalian topoisomerases and human thioredoxin reductase 1. Journal of Inorganic Biochemistry, 2009, 103, 1082-1092.	1.5	107
130	High-throughput screening of soluble recombinant proteins. Protein Science, 2009, 11, 1714-1719.	3.1	145
131	Unique GTP-Binding Pocket and Allostery of Uridylate Kinase from a Gram-Negative Phytopathogenic Bacterium. Journal of Molecular Biology, 2009, 385, 1113-1126.	2.0	10
132	Structure of the Alkalohyperthermophilic Archaeoglobus fulgidus Lipase Contains a Unique C-Terminal Domain Essential for Long-Chain Substrate Binding. Journal of Molecular Biology, 2009, 390, 672-685.	2.0	38
133	Insights into the Alkyl Peroxide Reduction Pathway of Xanthomonas campestris Bacterioferritin Comigratory Protein from the Trapped Intermediate–Ligand Complex Structures. Journal of Molecular Biology, 2009, 390, 951-966.	2.0	28
134	Inhibition of Staphyloxanthin Virulence Factor Biosynthesis in <i>Staphylococcus aureus</i> : In Vitro, in Vivo, and Crystallographic Results. Journal of Medicinal Chemistry, 2009, 52, 3869-3880.	2.9	106
135	Lipophilic Bisphosphonates as Dual Farnesyl/Geranylgeranyl Diphosphate Synthase Inhibitors: An X-ray and NMR Investigation. Journal of the American Chemical Society, 2009, 131, 5153-5162.	6.6	159
136	Anti-sense morpholino oligonucleotide assay shows critical involvement for NF-κB activation in the production of Wnt-1 protein by HepG2 cells: oncology implications. Journal of Biomedical Science, 2008, 15, 633-43.	2.6	4
137	Structures of a potent phenylalkyl bisphosphonate inhibitor bound to farnesyl and geranylgeranyl diphosphate synthases. Proteins: Structure, Function and Bioinformatics, 2008, 73, 431-439.	1.5	40
138	Crystal structure of DFA0005 complexed with αâ€ketoglutarate: A novel member of the ICL/PEPM superfamily from alkaliâ€ŧolerant <i>Deinococcus ficus</i> . Proteins: Structure, Function and Bioinformatics, 2008, 73, 362-371.	1.5	0
139	Right or left turn? RecA family protein filaments promote homologous recombination through clockwise axial rotation. BioEssays, 2008, 30, 48-56.	1.2	18
140	Discovery of virulence factors of pathogenic bacteria. Current Opinion in Chemical Biology, 2008, 12, 93-101.	2.8	191
141	Proteomics and genomics: perspectives on drug and target discovery. Current Opinion in Chemical Biology, 2008, 12, 1-3.	2.8	92
142	A Cholesterol Biosynthesis Inhibitor Blocks <i>Staphylococcus aureus</i> Virulence. Science, 2008, 319, 1391-1394.	6.0	422
143	Cysteine S-Nitrosylation Protects Protein-tyrosine Phosphatase 1B against Oxidation-induced Permanent Inactivation. Journal of Biological Chemistry, 2008, 283, 35265-35272.	1.6	135
144	Structural Basis for Catalytic and Inhibitory Mechanisms of Human Prostaglandin Reductase PTGR2. Structure, 2008, 16, 1714-1723.	1.6	46

#	Article	IF	CITATIONS
145	Crystal Structure of the C-Terminal Domain of a Flagellar Hook-Capping Protein from Xanthomonas campestris. Journal of Molecular Biology, 2008, 381, 189-199.	2.0	22
146	The First Crystal Structure of Gluconolactonase Important in the Glucose Secondary Metabolic Pathways. Journal of Molecular Biology, 2008, 384, 604-614.	2.0	31
147	Inhibition of Geranylgeranyl Diphosphate Synthase by Bisphosphonates: A Crystallographic and Computational Investigation. Journal of Medicinal Chemistry, 2008, 51, 5594-5607.	2.9	73
148	Precise Mapping of Increased Sialylation Pattern and the Expression of Acute Phase Proteins Accompanying Murine Tumor Progression in BALB/c Mouse by Integrated Sera Proteomics and Glycomics. Journal of Proteome Research, 2008, 7, 3293-3303.	1.8	27
149	Crystal structure of IcaR, a repressor of the TetR family implicated in biofilm formation in Staphylococcus epidermidis. Nucleic Acids Research, 2008, 36, 1567-1577.	6.5	64
150	White spot syndrome virus protein ICP11: A histone-binding DNA mimic that disrupts nucleosome assembly. Proceedings of the National Academy of Sciences of the United States of America, 2008, 105, 20758-20763.	3.3	79
151	A conserved hydrogen-bond network in the catalytic centre of animal glutaminyl cyclases is critical for catalysis. Biochemical Journal, 2008, 411, 181-190.	1.7	26
152	Structure-Based Inhibitors Exhibit Differential Activities against <i>Helicobacter pylori</i> and <i>Escherichia coli</i> Undecaprenyl Pyrophosphate Synthases. Journal of Biomedicine and Biotechnology, 2008, 2008, 1-6.	3.0	31
153	Taiwan proteomics society: an organization affiliated with HUPO. Molecular and Cellular Proteomics, 2008, 7, 1584-5.	2.5	Ο
154	White Spot Syndrome Virus Annexes a Shrimp STAT To Enhance Expression of the Immediate-Early Gene ie1. Journal of Virology, 2007, 81, 1461-1471.	1.5	188
155	Structure and Mechanism of Helicobacter pylori Fucosyltransferase. Journal of Biological Chemistry, 2007, 282, 9973-9982.	1.6	113
156	Crystal structure of the left-handed archaeal RadA helical filament: identification of a functional motif for controlling quaternary structures and enzymatic functions of RecA family proteins. Nucleic Acids Research, 2007, 35, 1787-1801.	6.5	40
157	Crystal Structures and Computer Screened Inhibitors of Helicobacter pylori Undecaprenyl Pyrophosphate Synthase. , 2007, , .		Ο
158	Identification of a Novel Prostaglandin Reductase Reveals the Involvement of Prostaglandin E2 Catabolism in Regulation of Peroxisome Proliferator-activated Receptor γ Activation. Journal of Biological Chemistry, 2007, 282, 18162-18172.	1.6	86
159	Chicken Heat Shock Protein 90 Is a Component of the Putative Cellular Receptor Complex of Infectious Bursal Disease Virus. Journal of Virology, 2007, 81, 8730-8741.	1.5	67
160	Protein expression profiling of the shrimp cellular response to white spot syndrome virus infection. Developmental and Comparative Immunology, 2007, 31, 672-686.	1.0	142
161	Structural basis of mercury―and zincâ€conjugated complexes as SARSâ€CoV 3Câ€like protease inhibitors. FEBS Letters, 2007, 581, 5454-5458.	1.3	51
162	Bisphosphonates target multiple sites in both cis- and trans-prenyltransferases. Proceedings of the National Academy of Sciences of the United States of America, 2007, 104, 10022-10027.	3.3	173

#	Article	IF	CITATIONS
163	Concerted Experimental Approach for Sequential Mapping of Peptides and Phosphopeptides Using C18-Functionalized Magnetic Nanoparticles. Journal of Proteome Research, 2007, 6, 1313-1324.	1.8	26
164	XC5848, an ORFan protein from Xanthomonas campestris, adopts a novel variant of Sm-like motif. Proteins: Structure, Function and Bioinformatics, 2007, 68, 1006-1010.	1.5	5
165	The crystal structure of XC1258 from <i>Xanthomonas campestris</i> : A putative procaryotic Nit protein with an arsenic adduct in the active site. Proteins: Structure, Function and Bioinformatics, 2007, 69, 665-671.	1.5	12
166	Structureâ€Based Design and Synthesis of Highly Potent SARSâ€CoV 3CL Protease Inhibitors. ChemBioChem, 2007, 8, 1654-1657.	1.3	33
167	Structural and Functional Analyses of Five Conserved Positively Charged Residues in the L1 and N-Terminal DNA Binding Motifs of Archaeal RadA Protein. PLoS ONE, 2007, 2, e858.	1.1	19
168	Synthesis, Crystal Structure, Structureâ^'Activity Relationships, and Antiviral Activity of a Potent SARS Coronavirus 3CL Protease Inhibitor. Journal of Medicinal Chemistry, 2006, 49, 4971-4980.	2.9	142
169	Crystal structure of infectious bursal disease virus VP2 subviral particle at 2.6Ã resolution: Implications in virion assembly and immunogenicity. Journal of Structural Biology, 2006, 155, 74-86.	1.3	61
170	2P592 Maturation and Mechanism Based Inhibitor Design of SARS-CoV 3CL Protease : Implication in Antiviral 3C(L) Protease Drug Design(55. Drug design and delivery,Poster Session,Abstract,Meeting) Tj ETQq0 0 () r gBT /Ov	erloock 10 Tf !
171	PL-5 Structural and functional analysis of enzyme targets for drug design(Plenary) Tj ETQq1 1 0.784314 rgBT /Ov	verlock 10 0.0k	Tf ₀ 50 422 To
172	1P195 Crystal structure of infectious bursal disease virus VP2 subviral particle : Implications in virion assembly and immunogenicity(6. Macromolecular assembly,Poster Session,Abstract,Meeting Program) Tj ETQq0	0 0. ogBT /	Oværlock 10
173	1P219 Structure of the left-handed archaeal RadA filament : a subunit rotation motif controls homologous DNA strand exchange reaction(7. Nucleic acid binding protein,Poster) Tj ETQq1 1 0.784314 rgBT /O	veolock 10) T 6 50 337 T
174	1P220 The DNA-recognition fold of Sso7c4 suggests an ancestral role in the evolution of β-barrel protein family(7. Nucleic acid binding protein,Poster Session,Abstract,Meeting Program of EABS & BSJ) Tj ETQq0	0 0. @BT /	Oværlock 10 ⁻
175	2P587 Inhibitors and maturation mechanism of SARS main protease(55. Drug design and delivery,Poster) Tj ETQ	1 0.784 0.0	13]4 rgBT /○
176	The crystal structure of XC1739: A putative multiple antibiotic-resistance repressor (MarR) from Xanthomonas campestris at 1.8 A resolution. Proteins: Structure, Function and Bioinformatics, 2006, 65, 239-242.	1.5	11
177	Crystal structure of XC5357 from Xanthomonas campestris: A putative tetracenomycin polyketide synthesis protein adopting a novel cupin subfamily structure. Proteins: Structure, Function and Bioinformatics, 2006, 65, 1046-1050.	1.5	4
178	Enzyme-substrate interactions revealed by the crystal structures of the archaeal Sulfolobus PTP-fold phosphatase and its phosphopeptide complexes. Proteins: Structure, Function and Bioinformatics, 2006, 66, 996-1003.	1.5	22
179	Dual binding sites for translocation catalysis by Escherichia coli glutathionylspermidine synthetase. EMBO Journal, 2006, 25, 5970-5982.	3.5	55
180	Kinetic and crystallographic studies of a redesigned manganese-binding site in cytochrome c peroxidase. Journal of Biological Inorganic Chemistry, 2006, 12, 126-137.	1.1	20

#	Article	IF	CITATIONS
181	Enhanced nuclear factor-kappa B-associated Wnt-1 expression in hepatitis B- and C-related hepatocarcinogenesis: identification by functional proteomics. Journal of Biomedical Science, 2006, 13, 27-39.	2.6	26
182	Identification of the Nucleocapsid, Tegument, and Envelope Proteins of the Shrimp White Spot Syndrome Virus Virion. Journal of Virology, 2006, 80, 3021-3029.	1.5	189
183	Photoreactivation of DNA by an Archaeal nucleoprotein Sso7d. Proceedings of the National Academy of Sciences of the United States of America, 2006, 103, 16655-16659.	3.3	24
184	Crystal Structure of Type-III Geranylgeranyl Pyrophosphate Synthase from Saccharomyces cerevisiae and the Mechanism of Product Chain Length Determination. Journal of Biological Chemistry, 2006, 281, 14991-15000.	1.6	99
185	DNA aptamers as potential anti-HIV agents. Trends in Biochemical Sciences, 2005, 30, 231-234.	3.7	70
186	A modified protein precipitation procedure for efficient removal of albumin from serum. Electrophoresis, 2005, 26, 2117-2127.	1.3	161
187	Design and characterization of a multimeric DNA binding protein using Sac7d and GCN4 as templates. Proteins: Structure, Function and Bioinformatics, 2005, 60, 617-628.	1.5	3
188	Biochemical and immunological studies of nucleocapsid proteins of severe acute respiratory syndrome and 229E human coronaviruses. Proteomics, 2005, 5, 925-937.	1.3	53
189	Crystal Structures of the BlaI Repressor from Staphylococcus aureus and Its Complex with DNA: Insights into Transcriptional Regulation of the bla and mec Operons. Journal of Bacteriology, 2005, 187, 1833-1844.	1.0	62
190	The Unique Stacked Rings in the Nucleocapsid of the White Spot Syndrome Virus Virion Are Formed by the Major Structural Protein VP664, the Largest Viral Structural Protein Ever Found. Journal of Virology, 2005, 79, 140-149.	1.5	72
191	Crystal Structures of Undecaprenyl Pyrophosphate Synthase in Complex with Magnesium, Isopentenyl Pyrophosphate, and Farnesyl Thiopyrophosphate. Journal of Biological Chemistry, 2005, 280, 20762-20774.	1.6	115
192	Homodimeric Hexaprenyl Pyrophosphate Synthase from the Thermoacidophilic Crenarchaeon Sulfolobus solfataricus Displays Asymmetric Subunit Structures. Journal of Bacteriology, 2005, 187, 8137-8148.	1.0	32
193	Mechanism of the Maturation Process of SARS-CoV 3CL Protease. Journal of Biological Chemistry, 2005, 280, 31257-31266.	1.6	215
194	Crystal structures of human glutaminyl cyclase, an enzyme responsible for protein N-terminal pyroglutamate formation. Proceedings of the National Academy of Sciences of the United States of America, 2005, 102, 13117-13122.	3.3	94
195	Substrate and product specificities of cis-type undecaprenyl pyrophosphate synthase. Biochemical Journal, 2005, 386, 169-176.	1.7	21
196	Mithramycin forms a stable dimeric complex by chelating with Fe(II): DNA-interacting characteristics, cellular permeation and cytotoxicity. Nucleic Acids Research, 2005, 33, 1352-1361.	6.5	25
197	Probing the DNA kink structure induced by the hyperthermophilic chromosomal protein Sac7d. Nucleic Acids Research, 2005, 33, 430-438.	6.5	36
198	Cloning, expression, characterization, and crystallization of a glutaminyl cyclase from human bone marrow: A single zinc metalloenzyme. Protein Expression and Purification, 2005, 43, 65-72.	0.6	26

#	Article	IF	CITATIONS
199	Self-cleavage of fusion protein in vivo using TEV protease to yield native protein. Protein Science, 2005, 14, 936-941.	3.1	50
200	Heterodimeric complexes of Hop2 and Mnd1 function with Dmc1 to promote meiotic homolog juxtaposition and strand assimilation. Proceedings of the National Academy of Sciences of the United States of America, 2004, 101, 10572-10577.	3.3	110
201	Genomic and Proteomic Analysis of Thirty-Nine Structural Proteins of Shrimp White Spot Syndrome Virus. Journal of Virology, 2004, 78, 11360-11370.	1.5	219
202	Crystal Structure of Octaprenyl Pyrophosphate Synthase from Hyperthermophilic Thermotoga maritima and Mechanism of Product Chain Length Determination. Journal of Biological Chemistry, 2004, 279, 4903-4912.	1.6	63
203	Crystal structure of the [Mg2+-(chromomycin A3)2]-d(TTGGCCAA)2 complex reveals GGCC binding specificity of the drug dimer chelated by a metal ion. Nucleic Acids Research, 2004, 32, 2214-2222.	6.5	78
204	The Functional Role of the Binuclear Metal Center in d-Aminoacylase. Journal of Biological Chemistry, 2004, 279, 13962-13967.	1.6	42
205	Crystal structures of the human SUMO-2 protein at 1.6â€fà and 1.2â€fà resolution. FEBS Journal, 2004, 271, 4114-4122.	0.2	62
206	Structures of Selenomonas ruminantium Phytase in Complex with Persulfated Phytate. Structure, 2004, 12, 2015-2024.	1.6	90
207	Substrate binding mode and reaction mechanism of undecaprenyl pyrophosphate synthase deduced from crystallographic studies. Protein Science, 2004, 13, 971-978.	3.1	54
208	Early detection of antibodies against various structural proteins of the SARS-associated coronavirus in SARS patients. Journal of Biomedical Science, 2004, 11, 117-126.	2.6	54
209	Structures of the hyperthermophilic chromosomal protein Sac7d in complex with DNA decamers. Acta Crystallographica Section D: Biological Crystallography, 2004, 60, 1381-1387.	2.5	13
210	Engineering a Thermostable Protein with Two DNA-binding Domains Using the Hyperthermophile Protein Sac7d. Journal of Biomolecular Structure and Dynamics, 2004, 21, 513-526.	2.0	6
211	In Vitro Modification of Human Centromere Protein CENP-C Fragments by Small Ubiquitin-like Modifier (SUMO) Protein. Journal of Biological Chemistry, 2004, 279, 39653-39662.	1.6	50
212	Self-polymerization of archaeal RadA protein into long and fine helical filaments. Biochemical and Biophysical Research Communications, 2004, 323, 845-851.	1.0	16
213	Immunological, structural, and preliminary X-ray diffraction characterizations of the fusion core of the SARS-coronavirus spike protein. Biochemical and Biophysical Research Communications, 2004, 324, 761-767.	1.0	9
214	Purification, crystallization and preliminary X-ray analysis of immunogenic virus-like particles formed by infectious bursal disease virus (IBDV) structural protein VP2. Acta Crystallographica Section D: Biological Crystallography, 2003, 59, 1234-1237.	2.5	6
215	Strategic shotgun proteomics approach for efficient construction of an expression map of targeted protein families in hepatoma cell lines. Proteomics, 2003, 3, 2472-2486.	1.3	89
216	Identification of the Active Conformation and the Importance of Length of the Flexible Loop 72â^'83 in Regulating the Conformational Change of Undecaprenyl Pyrophosphate Synthaseâ€. Biochemistry, 2003, 42, 14452-14459.	1.2	17

#	Article	IF	CITATIONS
217	The Refined Crystal Structure of an Eel Pout Type III Antifreeze Protein RD1 at 0.62-Ã Resolution Reveals Structural Microheterogeneity of Protein and Solvation. Biophysical Journal, 2003, 84, 1228-1237.	0.2	76
218	Catalytic Mechanism Revealed by the Crystal Structure of Undecaprenyl Pyrophosphate Synthase in Complex with Sulfate, Magnesium, and Triton. Journal of Biological Chemistry, 2003, 278, 29298-29307.	1.6	57
219	Crystal Structure of the Hyperthermophilic Archaeal DNA-Binding Protein Sso10b2 at a Resolution of 1.85 Angstroms. Journal of Bacteriology, 2003, 185, 4066-4073.	1.0	55
220	Crystal Structure of d-Aminoacylase from Alcaligenes faecalis DA1. Journal of Biological Chemistry, 2003, 278, 4957-4962.	1.6	54
221	Unusual DNA duplex and hairpin motifs. Nucleic Acids Research, 2003, 31, 2461-2474.	6.5	87
222	Crystal Structure of Yeast Cytosine Deaminase. Journal of Biological Chemistry, 2003, 278, 19111-19117.	1.6	113
223	Probing the Conformational Change of Escherichia coliUndecaprenyl Pyrophosphate Synthase during Catalysis Using an Inhibitor and Tryptophan Mutants. Journal of Biological Chemistry, 2002, 277, 7369-7376.	1.6	35
224	Crystal structure of actinomycin D bound to the CTG triplet repeat sequences linked to neurological diseases. Nucleic Acids Research, 2002, 30, 4910-4917.	6.5	60
225	Photoreactivity of 5-lodouracil-Containing DNA-Sso7d Complex in Solution:Â The Protein-Induced DNA Kink Causes Intrastrand Hydrogen Abstraction from the 5-Methyl of Thymine at the 5â€~ Side. Journal of the American Chemical Society, 2002, 124, 2086-2087.	6.6	22
226	The 1.35â€Ã structure of cadmium-substituted TM-3, a snake-venom metalloproteinase from Taiwan habu: elucidation of a TNFα-converting enzyme-like active-site structure with a distorted octahedral geometry of cadmium. Acta Crystallographica Section D: Biological Crystallography, 2002, 58, 1118-1128.	2.5	25
227	Determinants of the inhibition of a Taiwan habu venom metalloproteinase by its endogenous inhibitors revealed by X-ray crystallography and synthetic inhibitor analogues. FEBS Journal, 2002, 269, 3047-3056.	0.2	34
228	Structure, mechanism and function of prenyltransferases. FEBS Journal, 2002, 269, 3339-3354.	0.2	382
229	Mechanism of Product Chain Length Determination and the Role of a Flexible Loop in Escherichia coliUndecaprenyl-pyrophosphate Synthase Catalysis. Journal of Biological Chemistry, 2001, 276, 47474-47482.	1.6	90
230	Crystal structures of the chromosomal proteins Sso7d/Sac7d bound to DNA containing T-G mismatched base-pairs. Journal of Molecular Biology, 2000, 303, 395-403.	2.0	55
231	Structural studies of atom-specific anticancer drugs acting on DNA. , 1999, 83, 181-215.		192
232	High-resolution A-DNA crystal structures of d(AGGGGCCCCT). An A-DNA model of poly(dG).poly(dC). FEBS Journal, 1999, 261, 413-420.	0.2	39
233	Binding of AR-1-144, a tri-imidazole DNA minor groove binder, to CCGG sequence analyzed by NMR spectroscopy. FEBS Journal, 1999, 263, 646-655.	0.2	24
234	Structural Basis of Electron Transfer Modulation in the Purple CuACenterâ€. Biochemistry, 1999, 38, 5677-5683.	1.2	90

#	Article	IF	CITATIONS
235	The Solution Structure of the Sac7d/DNA Complex: A Small-Angle X-ray Scattering Studyâ€. Biochemistry, 1999, 38, 10247-10255.	1.2	32
236	Solution Structure of a DNA Duplex Containing acis-Diammineplatinum(II) 1,3-d(GTG) Intrastrand Cross-Link, a Major Adduct in Cells Treated with the Anticancer Drug Carboplatinâ€. Biochemistry, 1999, 38, 12305-12312.	1.2	75
237	The hyperthermophile chromosomal protein Sac7d sharply kinks DNA. Nature, 1998, 392, 202-205.	13.7	208
238	The crystal structure of the hyperthermophile chromosomal protein Sso7d bound to DNA. Nature Structural Biology, 1998, 5, 782-786.	9.7	136
239	Monofunctional platinum amine complexes destabilize DNA significantly. FEBS Journal, 1998, 256, 253-260.	0.2	35
240	DNA Interactions of Two Clinical Camptothecin Drugs Stabilize Their Active Lactone Forms. Journal of the American Chemical Society, 1998, 120, 2979-2980.	6.6	72
241	Structural Studies of a Stable Parallel-Stranded DNA Duplex Incorporating Isoguanine:Cytosine and Isocytosine:Guanine Basepairs by Nuclear Magnetic Resonance Spectroscopy. Biophysical Journal, 1998, 75, 1163-1171.	0.2	55
242	Molecular Structure of Two Crystal Forms of Cyclic Triadenylic Acid at 1Ã Resolution. Journal of Biomolecular Structure and Dynamics, 1998, 16, 69-76.	2.0	4
243	Binding of Daunorubicin to β-d-Glucosylated DNA Found in Protozoa Tryponosoma brucei Studied by X-ray Crystallography. Journal of the American Chemical Society, 1997, 119, 1496-1497.	6.6	27
244	Structures of Cobalt(III)-Pepleomycin and Cobalt(III)-Deglycopepleomycin (green forms) Determined by NMR Studies. FEBS Journal, 1997, 244, 818-828.	0.2	41
245	Analyses of the stability and function of three surface mutants (R82C, K69H, and L32R) of the gene V protein from Ff phage by Xâ€ray crystallography. Protein Science, 1997, 6, 771-780.	3.1	13
246	Bridged cobalt amine complexes induce DNA conformational changes effectively. Journal of Inorganic Biochemistry, 1997, 68, 129-135.	1.5	19
247	Deoxyadenosine and Thymidine Bases Held Proximal and Distal by Means of a Covalently-Linked Dimensional Analogue of dA·dT: Intramolecular vs Intermolecular Hydrogen Bonding1. Journal of the American Chemical Society, 1996, 118, 10744-10751.	6.6	34
248	2â€~-Deoxy-3-isoadenosine Forms Hoogsteen-Type Base Pairs with Thymidine in the d(CG[iA]TCG)2 Duplex1. Journal of the American Chemical Society, 1996, 118, 3065-3066.	6.6	11
249	Binding of the Antitumor Drug Nogalamycin to Bulged DNA Structuresâ€. Biochemistry, 1996, 35, 616-625.	1.2	23
250	Structure of Actinomycin D bound with (GAAGCTTC)2and (GATGCTTC)2and Its Binding to the (CAG)n:(CTG)nTriplet Sequence As Determined by NMR Analysisâ€. Journal of the American Chemical Society, 1996, 118, 8791-8801.	6.6	47
251	Context Dependence of Mutational Effects in a Protein: The Crystal Structures of the V35I, I47V and V35I/I47V Gene V Protein Core Mutants. Journal of Molecular Biology, 1996, 259, 148-159.	2.0	21
252	Interaction between left-handed Z-DNA and polyamine - 3 The crystal structure of the d(CG)3and thermospermine complex. FEBS Letters, 1996, 398, 291-296.	1.3	23

#	Article	IF	CITATIONS
253	Synthesis, Structure and Thermodynamic Properties of 8-Methylguanine-Containing Oligonucleotides: Z-DNA under Physiological Salt Conditions. Nucleic Acids Research, 1996, 24, 1272-1278.	6.5	101
254	Substitutions at C2' of Daunosamine in the Anticancer Drug Daunorubicin Alter Its DNA-Binding Sequence Specificity. FEBS Journal, 1996, 240, 331-335.	0.2	9
255	Structural studies of interactions between anticancer platinum drugs and DNA. Progress in Biophysics and Molecular Biology, 1996, 66, 81-111.	1.4	56
256	Structural Effect of Intra-strand Cisplatin-crosslink on Palindromic DNA Sequences. Journal of Biomolecular Structure and Dynamics, 1996, 13, 989-998.	2.0	27
257	A novel DNA structure induced by the anticancer bisplatinum compound crosslinked to a GpC site in DNA. Nature Structural Biology, 1995, 2, 577-586.	9.7	56
258	Crystal Structures of Four Morpholino-Doxorubicin Anticancer Drugs Complexed with d(CGTACG) and d(CGATCG): Implications in Drug-DNA Crosslink. Journal of Biomolecular Structure and Dynamics, 1995, 13, 103-117.	2.0	18
259	DNA with 2'-5' Phosphodiester Bonds Forms a Duplex Structure in the A-type Conformation. Journal of the American Chemical Society, 1995, 117, 837-838.	6.6	43
260	Electrostatic potential distribution of the gene V protein from Ff phage facilitates cooperative DNA binding: A model of the GVPâ€ssDNA complex. Protein Science, 1995, 4, 187-197.	3.1	24
261	Human chromosomal centromere (AATGG)n sequence forms stable structures with unusual base pairs. FEBS Letters, 1994, 347, 99-103.	1.3	7
262	Conformations of the alternating (C-T)nsequence under neutral and low pH. FEBS Letters, 1994, 337, 139-144.	1.3	5
263	Structure and dynamics of the antitumor drugs nogalamycin and disnogalamycin complexed to d(CGTACG)2: comparison of crystal and solution structures. Gene, 1994, 149, 179-188.	1.0	11
264	5'-CGA Motif Induces Other Sequences To Form Homo Base-Paired Parallel-Stranded DNA Duplex: The Structure of (G-A)n Derived from Four DNA Oligomers Containing (G-A)3 Sequence. Journal of the American Chemical Society, 1994, 116, 1565-1566.	6.6	30
265	Adducts of DNA and Anthracycline Antibiotics. ACS Symposium Series, 1994, , 168-182.	0.5	4
266	Crystallographic studies of metal ion - DNA interactions: different binding modes of cobalt(II), copper(II) and barium(II) to N7of guanines in Z-DNA and a drug-DNA complex. Nucleic Acids Research, 1993, 21, 4093-4101.	6.5	137
267	NMR studies of pH-dependent conformational polymorphism of alternating (C-T)n sequences. Nucleic Acids Research, 1993, 21, 3839-3844.	6.5	21
268	Molecular Structure of Cyclic Diguanylic Acid at 1 Ã Resolution of Two Crystal Forms: Self-association, Interactions with Metal Ion/Planar Dyes and Modeling Studies. Journal of Biomolecular Structure and Dynamics, 1993, 11, 253-276.	2.0	21
269	Studies on 1,2,4-Benzothiadiazine 1,1-Dioxides VII and Quinazolinones IV: Synthesis of Novel Built-In Hydroxyguanidine Tricycles as Potential Anticancer Agents. Heterocycles, 1993, 36, 1091.	0.4	29
270	Unusual conformational flexibility in N1-substituted uncommon purine nucleosides Crystal structure of 1-allyl-isoguanosine and 1-allyl-xanthosine. FEBS Letters, 1992, 297, 4-8.	1.3	5

#	Article	IF	CITATIONS
271	Conformational perturbation of the anticancer nucleoside arabinosylcytosine on Z-DNA: Molecular structure of (araC-dG)3at 1.3 Ã resolution. Biopolymers, 1992, 32, 1559-1569.	1.2	13
272	Interaction between the left-handed Z-DNA and polyamine The crystal structure of the d(CG)3andN-(2-aminoethyl)-1,4-diamino-butane complex. FEBS Letters, 1991, 284, 238-244.	1.3	31
273	Molecular Structure of Antitumor Drug Steffimycin and Modelling of its Binding to DNA. Journal of Biomolecular Structure and Dynamics, 1991, 9, 251-269.	2.0	6
274	NMR studies on the binding of antitumor drug nogalamycin to DNA hexamer d(CGTACG). Nucleic Acids Research, 1990, 18, 4851-4858.	6.5	38
275	Molecular Structure of the Complex Formed Between the Anticancer Drug Cisplatin and d(pCpG): C222 ₁ Crystal Form. Journal of Biomolecular Structure and Dynamics, 1990, 8, 315-330.	2.0	43
276	Structure of 11-deoxydaunomycin bound to DNA containing a phosphorothioate. Journal of Molecular Biology, 1990, 215, 313-320.	2.0	36
277	Cyclic diguanylic acid behaves as a host molecule for planar intercalators. FEBS Letters, 1990, 264, 223-227.	1.3	35
278	Interactions Between a Symmetrical Minor Groove Binding Compound and DNA Oligonucleotides: 1H and 19F NMR Studies. Journal of Biomolecular Structure and Dynamics, 1989, 7, 101-117.	2.0	8
279	The propeller DNA conformation of poly(dA).poly(dT). Nucleic Acids Research, 1989, 17, 3229-3245.	6.5	67
280	Molecular structure of an A-DNA decamer d(ACCGGCCGGT). FEBS Journal, 1989, 181, 295-307.	0.2	57
281	Preliminary crystallographic studies of the Fab fragment of an anti-azophenylarsonate antibody. Journal of Molecular Biology, 1989, 206, 789-790.	2.0	1
282	Effects of 5-fluorouracil/guanine wobble base pairs in Z-DNA: molecular and crystal structure of d(CGCGFG). Nucleic Acids Research, 1989, 17, 911-923.	6.5	32
283	Crystallization and crystal packing analysis of DNA oligonucleotides. Journal of Crystal Growth, 1988, 90, 295-310.	0.7	21
284	Crystallization of a small fragment of an aminoacyl tRNA synthetase. Journal of Molecular Biology, 1988, 203, 521-522.	2.0	14
285	Local mobility of nucleic acids as determined from crystallographic data. Journal of Molecular Biology, 1988, 199, 349-357.	2.0	23
286	The molecular structure of the complex of Hoechst 33258 and the DNA dodecamer d(CGCGAATTCGCG). Nucleic Acids Research, 1988, 16, 2671-2690.	6.5	335
287	The Interactions of Ruthenium Hexaammine with Z-DNA: Crystal Structure of a RU(NH ³) ⁺³ ₆ Salt of d(CGCGCC) at 1.2 Ã Resolution. Journal of Biomolecular Structure and Dynamics, 1987, 4, 521-534.	2.0	73
288	The crystal structure of d(GGm5CCGGCC): The effect of methylation on A-DNA structure and stability. Biopolymers, 1987, 26, S145-S160.	1.2	31

#	Article	IF	CITATIONS
289	Local mobility of nucleic acids as determined from crystallographic data. Journal of Molecular Biology, 1986, 187, 429-440.	2.0	24
290	Interactions of Quinoxaline Antibiotic and DNA.: The Molecular Structure of a Triostin A—d(GCGTACGC) Complex. Journal of Biomolecular Structure and Dynamics, 1986, 4, 319-342.	2.0	65
291	Crystal Structure of A Z-DNA Fragment Containing Thymine/2-Aminoadenine Base Pairs. Journal of Biomolecular Structure and Dynamics, 1986, 4, 157-172.	2.0	34
292	The octamers d(CGCGCGCG) and d(CGCATGCG) both crystallize as Z-DNA in the same hexagonal lattice. Biopolymers, 1985, 24, 243-250.	1.2	61
293	31P-NMR analysis of the B to Z transition in double-stranded (dC-dG)3, and (dC-dG)4in high salt solution. Nucleic Acids Research, 1984, 12, 4625-4635.	6.5	23
294	A one- and two-dimensional NMR study of the B to Z transition of (m5dC-dG)3in methanolic solution. Nucleic Acids Research, 1984, 12, 1243-1263.	6.5	130
295	Conformation and Dynamics of Short DNA Duplexes: (dC-dG)3and (dC-dG)4. Journal of Biomolecular Structure and Dynamics, 1984, 1, 1373-1386.	2.0	23
296	Conformation of Nucleic Acids and Their Interactions with Drugs. ACS Symposium Series, 1984, , 105-136.	0.5	0
297	AT base pairs are less stable than GC base pairs in Z-DNA: The crystal structure of d(m5CGTAm5CG). Cell, 1984, 37, 321-331.	13.5	211
298	Molecular structure of (m5dC-dG)3: the role of the methyl group on 5-methyl cytosine in stabilizing Z-DNA. Nucleic Acids Research, 1982, 10, 7879-7892.	6.5	203
299	Molecular structure of r(GCG)d(TATACGC): a DNA–RNA hybrid helix joined to double helical DNA. Nature, 1982, 299, 601-604.	13.7	223
300	Atomic resolution analysis of a 2:1 complex of CpG and acridine orange. Nucleic Acids Research, 1979, 6, 3879-3890.	6.5	66
301	Molecular structure of a left-handed double helical DNA fragment at atomic resolution. Nature, 1979, 282, 680-686.	13.7	2,099
302	A crystallographic investigation of citrate synthase from pig and chicken heart muscle. Biochemical and Biophysical Research Communications, 1978, 82, 150-156.	1.0	6
303	Crystallographic studies of a mitogenic lectin from pea seeds. Biochemical and Biophysical Research Communications, 1977, 76, 1261-1266.	1.0	3
304	Barbatusin and cyclobutatusin, two novel diterpenoids from coleus barbatus bentham. Tetrahedron, 1977, 33, 1457-1467.	1.0	38
305	Solid state structure of two iron carbonyl complexes derived from barbaralone and the isobullvalene ring skeleton. Characterization of a possible "homobutadiene—Fe(CO)3―complex. Journal of Organometallic Chemistry, 1974, 69, 301-304.	0.8	22